INDUCTIVELY DRIVEN TRANSIENTS IN THE CS INSERT COIL (I): HEATER CALIBRATION AND CONDUCTOR STABILITY TESTS AND ANALYSIS

R. Zanino[@], E. Carpaneto[#], A. Portone[$], E. Salpietro[$] and L. Savoldi[@]

[@] Dipartimento di Energetica, Politecnico,
Torino, I-10129 Italy

[#] Dipartimento di Ingegneria Elettrica Industriale, Politecnico,
Torino, I-10129 Italy

[$] EFDA, Garching, Germany

ABSTRACT

The CS Insert Coil (CSIC), a well-instrumented 140 m long Nb_3Sn solenoid wound one-in-hand and installed in the bore of the CS Model Coil, was tested during the summer of 2000 at JAERI Naka, Japan, within the framework of the International Thermonuclear Experimental Reactor large projects [1]. The maximum transport current in the CSIC was 40 kA and the peak background field was 13 T. The coils were cooled by forced flow HeI nominally at 4.5 K and 0.6 MPa. An inductive heater was used to study stability and quench propagation in the CSIC. In this first of two companion papers we concentrate on the conductor stability tests, while a second paper is dedicated to the analysis of quench propagation [2]. The stability margin of the conductor was measured for different transport currents, helium mass flow rates and temperature margins, and the corresponding results will be presented and discussed. In the analysis, a major uncertainty comes from the assessment of the actual energy input and its partition between jacket and cable. Therefore, an electromagnetic model of the inductive heater was developed and validated. Using this input, the stability margin is computed with the Mithrandir code and compared with experimental results, showing good agreement.

INTRODUCTION AND EXPERIMENTAL SETUP

The stability of the CSIC was tested using one of the four inductive heaters (IH), installed on the central turn of the conductor, i.e., at the maximum magnetic field. The IH was a copper solenoid wound around the thick square Incoloy jacket (~ 51 mm side, ~ 38 mm inner diameter) of the conductor, over a total length of ~ 109 mm. For different transport current,

CP613, *Advances in Cryogenic Engineering: Proceedings of the Cryogenic Engineering Conference, Vol. 47,*
edited by Susan Breon et al.
© 2002 American Institute of Physics 0-7354-0059-8/02/$19.00

initial temperature and helium mass flow rate in the CSIC, a 20 ms 1 kHz current pulse $I_h(t)$ was circulated in the IH, discharging a series of capacitors over the heater. In order to experimentally assess the stability of the conductor, the voltage drop applied to the heater was increased step by step until a quench occurred. The initiation of a normal zone was revealed by voltage taps distributed along the conductor and concentrated in the central turn where the heater is located. In FIG 1 a collection of the measured stability data is reported in terms of the $\int I_h^2 dt$ leading to a quench (solid symbols) and of the $\int I_h^2 dt$ for which the conductor either does not quench or recovers the superconducting state (open symbols). The stability (or energy) margin can then be defined as the average between minimum energy for quench and maximum energy for no quench/recovery. Notice that $\int I_h^2 dt$ is proportional to the energy E deposited by the IH into the conductor at constant applied voltage frequency. The proportionality factor C_H, where

$$C_H = E / \int I_h^2 dt,$$

is not known a priori but it can be experimentally determined by "calibration".

The dependence of the energy margin on the transport current *I* (FIG 1a) is obviously due to the fact that the critical temperature decreases as the operating current density increases. Similarly, as to the influence of the temperature margin ($T_{cs} - T$), it is clear that an increase of the operating temperature T towards the current sharing temperature T_{cs}, i.e., a

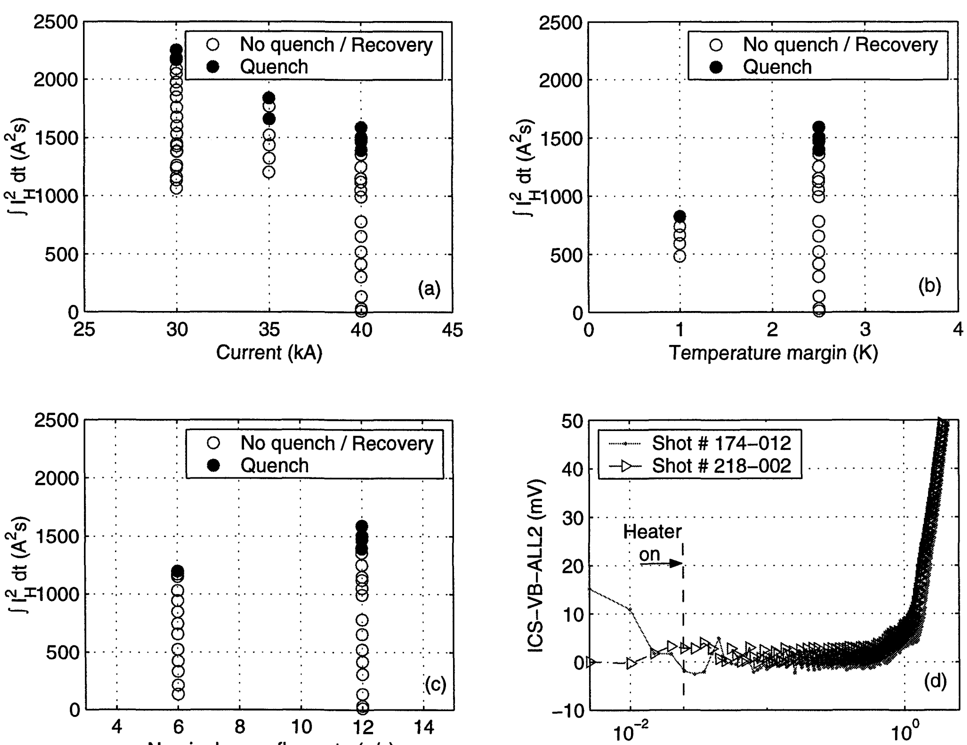

FIGURE 1. Experimental results of stability and quench tests: (a) threshold as a function of transport current @ 12 g/s, and $\Delta T_{margin} = 2.5$ K, (b) threshold as a function of ΔT_{margin} @ 40 kA and 12 g/s, (c) threshold as a function of nominal mass-flow rate @ 40 kA and $\Delta T_{margin} = 2.5$ K, (d) balanced voltage evolution when the quench is reached @ 40 kA, 12 g/s, and $\Delta T_{margin} = 2.5$ K (shots # 174-012 – stability test – and 218-002 – quench test). When more than one quench point is present for given conditions (notice a spread up to 10 %), this corresponds to different shots in the campaign.

reduction of the temperature margin, means that a smaller energy input is needed to initiate a quench (FIG 1b). Finally, it may be noticed that there is a weak dependence on the initial mass flow rate (FIG 1c), leading to a slight increase of the energy margin for a doubling of (dm/dt).

A peculiarity of the IH stability tests, see FIG 1d, is that the take-off of the resistive voltage along the cable does not start during the (20 ms) heating, but on a much longer (~1 s) time scale. This is a clear indication that the IH deposits most of the energy into the Incoloy jacket, because of its significant thickness (see FIG 2), while the strands are heated mainly indirectly, by conduction from the jacket and convection from the bundle helium. (This feature is obviously undesired, since the original purpose of using an *inductive*, as opposed to a resistive, heater was to deposit energy *directly into the strands*, in attempt to simulate their internal motion.) Indeed, the calibration of the IH, performed several months after the CSIC tests [3], confirmed this observation. The parameter χ_H, where

$$\chi_H = \text{energy deposited in the strands} / E$$

was estimated to be ~ 5% [3]. From the same tests C_H was also estimated within a 10% accuracy to be ~ 0.155 J/A^2s.

The thermal-hydraulic transients in the 2-channel CICC conductors, such as the CSIC, can be studied by means of computational tools, e.g. the Mithrandir code [4], which was already validated against heat-slug [5] and quench [6] transients in QUELL. In order to attempt computing the stability margin with Mithrandir, however, it is not sufficient to have an accurate estimation of the total energy deposited in the jacket and in the strands (or cable) region, but it is mandatory to know its time evolution and space distribution.

For a proper description of the heat deposition during inductive heating, a model of the IH heater has been developed and validated against data from [3]. The computed power distribution in cable and jacket has been used as input for the Mithrandir code, to assess the stability margin in several different conditions, and the results are compared with the measured values.

As a word of caution, it is worth mentioning finally that the analysis of the pressure drop in the CSIC [7] shows that the Lorentz forces acting on the conductor at maximum current and field probably caused some displacement/deformation of the cable. Since this effect is not taken into account in our model, except for the use of a friction factor which was developed ad-hoc [8], it is not possible here to assess what other influence this could have had on quench initiation and propagation in the CSIC.

ELECTROMAGNETIC MODEL OF THE INDUCTIVE HEATER

A simplified 2D electromagnetic model of the inductive heater (see FIG 2) has been developed. Purpose of the model is to compute the distribution in time and space of the power deposited by the heater into cable and jacket, using the waveform of the current in the heater as input.

The model is first calibrated and then validated against experimental results obtained at JAERI [3], testing calorimetrically different samples. These include: 1) heater only, 2) heater + cable, 3) heater + jacket, and 4) heater + conductor (= cable + jacket).

In the model (FIG 2b) it is assumed that the inductive heater, the jacket and the cable have a cylindrical geometry with symmetry axis along the longitudinal (Z) direction, and only a limited length (ΔZ=200 mm) of the jacket and cable needs to be analyzed. As for the assumption of cylindrical symmetry around Z, it must be remarked that, in reality, the actual

IH and jacket cross section is approximately square (FIG 2a), which would require a relatively cumbersome 3D model. On the other hand we do not expect this assumption to change substantially the results provided that the IH and jacket outer diameter in the model are adequately chosen as described hereafter.

The heater is modeled as a 109 mm long solenoid made by a Cu wire with a diameter of 1.6 mm, an insulation layer 0.075 mm thick and wound in 59 turns around the jacket outer cylindrical surface. The IH average diameter ($\approx$ 60 mm) has been chosen to preserve the total IH cross-section area and therefore approximately the same longitudinal field on the cable and jacket cross-section.

The jacket is modeled with inner and outer diameter 38.5 mm (coinciding with the actual value) and 52 mm, respectively. The latter figure was obtained by preserving the jacket Joule losses measured during an IH calibration experiment at 2 T (shot 061_06, [3]) in which only the IH and the jacket are present. It should be noted that the outer diameter obtained from this constraint corresponds approximately to the smallest thickness of the actual square jacket, somehow implying that the currents flowing in the corners of the jacket cross-section give a limited contribution to the Joule losses. The model assumes that the current in the jacket flows only in the azimuthal (φ) direction. The measured electrical resistivity at 4 K of the Incoloy jacket after the thermal heat treatment is η_j=0.93 $\mu\Omega$ m [8]. The magnetic permeability is assumed equal to that of vacuum ($\mu=\mu_0=4\pi \times 10^{-7}$ H/m) since the background field (2-13 T) is typically well above the Incoloy saturation field ($\approx$ 1 T) and the field variation due to the IH current is small ($\approx$ 0.1 T) compared to such values.

The cable is modeled similarly to the jacket. For the sake of simplicity it is assumed to be a homogeneous, solid conductor, i.e., no strands or bundles of strands are considered. The inner boundary at the outer surface of the central cooling channel has a diameter of 12 mm whereas the outer boundary coincides with the jacket inner surface. The major difference with respect to the jacket is that, in an attempt to roughly simulate current flow in the cable cross section, with the petals insulated from each other by the sub-cable wraps, we force the *total* azimuthal current in the cable to vanish. The cable *effective* electrical resistivity at 4 K is η_c=0.8 $\mu\Omega$ m. This value was obtained by fitting the Joule losses in the cable measured during two IH calibration experiments at 2 T (shots 055_06 and 078_06, [3]) in which only the IH and the cable are present. Since the resistive current paths in the cable flow - primarily - in the copper, this effective electrical resistivity has been assumed to scale with the external magnetic field similarly to the one of copper (with RRR=100), leading to η_c(4 T)=1.1 $\mu\Omega$ m and η_c(13 T)=2.4 $\mu\Omega$ m. As for the magnetic permeability, also in the cable $\mu=\mu_0$.

From the electrical standpoint, each of the rectangles in the model of FIG 2 represents a circuit to which we associate a resistance, a (self-)inductance and mutual inductances,

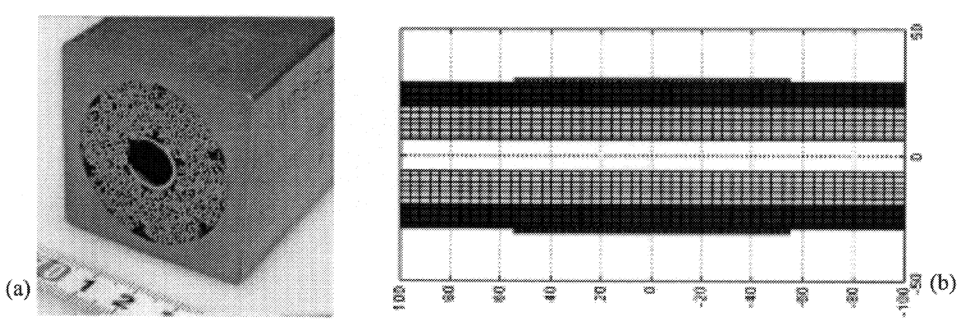

FIGURE 2. (a) CSIC conductor (courtesy of JAERI). (b) Cylindrical (R,Z) electromagnetic model of the longitudinal cross section of the CSIC IH and conductor, with dimensions in mm: in this particular case the jacket is discretized in 50×4 azimuthal current loops of rectangular cross section, in the Z (R) direction respectively, the cable in 50×6 similar loops.

TABLE 1. Comparison between calorimetric data and electro-magnetic model results

Shot number	080_05	065_05	085_05	067_05	089_05
Circuits present in the sample (IH=heater, J=Jacket, C=Cable)	IH+C	IH+J+C	IH+J+C	IH+J+C	IH+J+C
Background magnetic field (T)	4	2	2	4	4
Effective cable resistivity ($\mu\Omega$ m)	1.1	0.8	0.8	1.1	1.1
$\int I_h^2$ (t) dt (A^2s)	309	177	207	156	167
Total energy dissipated (measured) (J)	29	25	32	28	32
Joule energy in J+C or C (experiment) (J)	7	21	27	17	21
Joule energy in J+C or C (simulation) (J)	9	25	29	22	24
Error (computed vs. measured) (%)	29	19	7	29	14

which can all be computed analytically using standard formulas, and the additional constraint that the *total* azimuthal current *in the cable* is zero is enforced. The current distribution in the jacket and cable, is then obtained by solving the resulting R-L network, described by the linear circuit equations:

$$\begin{bmatrix} \mathbf{L}_{jj} & \mathbf{M}_{jc} \\ \mathbf{M}_{cj} & \mathbf{L}_{cc} \end{bmatrix} \begin{bmatrix} \dot{\mathbf{I}}_j \\ \dot{\mathbf{I}}_c \end{bmatrix} + \begin{bmatrix} \mathbf{R}_j & \mathbf{0} \\ \mathbf{0} & \mathbf{R}_c \end{bmatrix} \begin{bmatrix} \mathbf{I}_j \\ \mathbf{I}_c \end{bmatrix} = -\begin{bmatrix} \mathbf{M}_{jh} \\ \mathbf{M}_{ch} \end{bmatrix} \dot{I}_h$$

in which the heater current $I_h(t)$ is the known driver. In the case of FIG 2 the sub-matrices $\mathbf{L}_{jj}$, $\mathbf{R}_j$ have dimension 200x200, while $\mathbf{L}_{cc}$, $\mathbf{R}_c$ are 299x299. The original 300 unknown currents in the cable reduce in fact to 299, once the above-mentioned constraint of total zero current in the cable has been enforced.

The power deposition computed by the model turns out typically to be concentrated in the outermost layer of the jacket.

VALIDATION AND APPLICATION OF THE INDUCTIVE HEATER MODEL

The results of the calibrated electromagnetic model described above have been compared with the results of a series of experiments performed on different types of sample, and in particular samples where only heater + cable or else heater + conductor were present. In these experiments the energy dissipated on R_h, $\mathbf{R}_j$ and $\mathbf{R}_c$ was measured calorimetrically [3]. The validation has been carried out for the experimental set-ups presented in TABLE 1, where also the main input data and results are reported. In particular, the average error in the Joule energy computed by the model, compared to that derived from the experimental data, turns out to be $\approx$ 20%.

Finally, the electromagnetic model described here has been used to predict the Joule losses in cable and jacket in three CSIC shots at 13 T (174-008, 174-011, 174-012). The main results of the simulations are reported in TABLE 2.Both C_H and χ_H as computed from the model are very close to the above-mentioned values (0.155 J/A^2s and 5% respectively) estimated from the heater calibration samples [3].

TABLE 2. Results of the application of the electro-magnetic model to the CSIC

CSIC shot number	174-008	174-011	174-012
$\int I_h^2$ (t) dt (A^2s)	656	1151	1393
Joule energy in Jacket/Cable (J)	87/5	152/8	183/10
C_H (J/A^2s)	0.140	0.139	0.139
χ_H (%)	5.4	5.0	5.2

ANALYSIS OF THE CSIC STABILITY TEST

The model implemented in the Mithrandir code is 1-D along the conductor axis, and the jacket temperature is assumed to be uniform over the cross section. Since, however, the power deposition in the jacket is not uniform, the jacket under the heater has been treated here with a *radial* 1D model. This allows for a temperature gradient in the jacket, which then leads to an improved, although still simplified modeling of heat transfer from the jacket to the bundle region. The total cross section area of the jacket has been preserved taking an outer diameter of ~ 58 mm, because the total heat capacity must be conserved, while the heat computed from the IH model has been deposited only in the innermost layers, up to a diameter of 52 mm (see previous sections).

The present simulations have been performed with Mithrandir using the geometrical parameters of the CSIC conductor as in [7], and a simplified external hydraulic circuit to provide the boundary conditions. From the point of view of the thermal-hydraulic input parameters, the friction factor in the hole and bundle regions has been adopted as in [7]. More delicate is the problem of the various heat transfer mechanisms/coefficients, which may be relevant in a CICC. Here, looking for an *integrated* optimization of both stability and quench results, we have come up with constant steady-state heat transfer coefficients between helium and jacket and between helium and strands, both ~ 5000 W/m^{2}K, and effective heat transfer coefficient between hole and bundle helium ~ 1000 W/m^{2}K. The contact heat transfer coefficient between strands and jacket is assumed to be ~ 500 W/m^{2}K. Notice that heat transfer

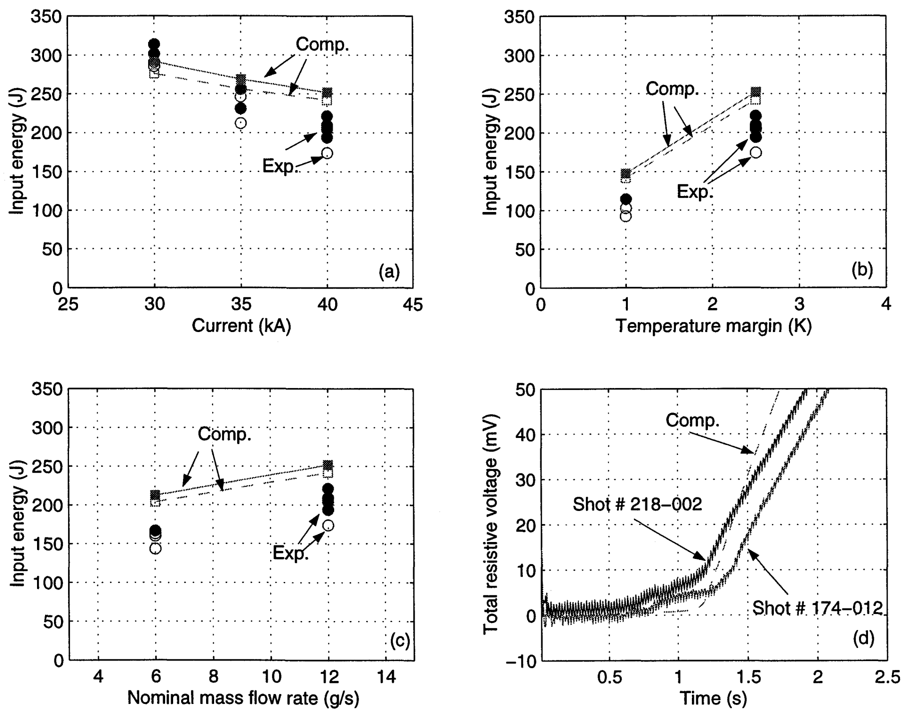

FIGURE 3. Comparison between Mithrandir simulation and experimental results: (a) energy margin as a function of transport current @ 12 g/s, and ΔT_{margin} = 2.5 K, (b) energy margin as a function of ΔT_{margin} @ 40 kA and 12 g/s, (c) energy margin as a function of nominal mass-flow rate @ 40 kA and ΔT_{margin} = 2.5 K, (d) balanced voltage evolution when the quench is reached @ 40 kA, 12 g/s, and ΔT_{margin} = 2.5 K (shots # 174-012 – stability test – and 218-002 – quench test). Experimental data in terms of $\int I_h^2\,dt$ (A^2 s) have been translated in energy (J) using the calibration of the IH model.

coefficients of the order of ~ 5000 W/m^2K, or even larger, can be justified in principle using for the cable bundle region correlations for the Nusselt number developed from packed-bed (porous medium) data (see [9] and references therein).

The critical superconductor parameters adopted for the simulations are: $C_0 = 0.98 \times 10^{10}$ AT/m^2, T_{c0m}=17.8 K, B_{c20m} = 30.2 T. The n-value in the *V-I* characteristic of the cable has been shown from experimental results to be reduced from the measured strand value [10], and n = 7.5 is adopted here. We choose $\varepsilon = -0.27\%$ as the value of the longitudinal strain in the conductor [10,11]. The magnetic field distribution along the CSIC was obtained from [12]. RRR = 140.

Notice finally that, in Mithrandir, a uniform current distribution among the strands is assumed. The extent to which this assumption is justified in the CSIC is currently under discussion [10,13-14], so that it may be interesting to see what accuracy can be achieved by the code results vs. the experiment, relying on this simplifying hypothesis.

It may be noticed from FIG 3 that the major trends of the experimental data are reproduced by the code results, and that even quantitatively the agreement is reasonable, considering the number of uncertainties (e.g., the above-mentioned ~ 20 % accuracy in the determination of the actual input energy) present in this problem.

In view of the above-mentioned uncertainties in the heat transfer coefficient h between helium and solids, we have also performed a preliminary sensitivity study, which is reported in FIG 4.

From FIG 4a and FIG 4b it may be noticed that a *reduction* of a factor 5 in h, down to the more customary value of 1000 W/m^2K, leads to an average *increase* of the energy margin by ~ 20 %, which goes away from the experimental results. The reason for this dependence is that here the strands are *heated* from the helium, which is in turn heated from the jacket. For the same finite effective duration of the heating pulse, which is here of the order of the transit time of helium under the IH, a reduction of h gives therefore a smaller effective energy deposition into the (cold) strands. Therefore, the strands need a higher energy input from the IH for the normal transition. (This is somewhat counterintuitive, because one normally thinks of the h as speeding-up the *cooling* of the warm strands.)

It may be finally remarked that a reduction of h leads to a significantly faster quench propagation (not shown). In the frame of an integrated stability/quench study like the present one, this was also an important reason to choose the reference parameter values used here.

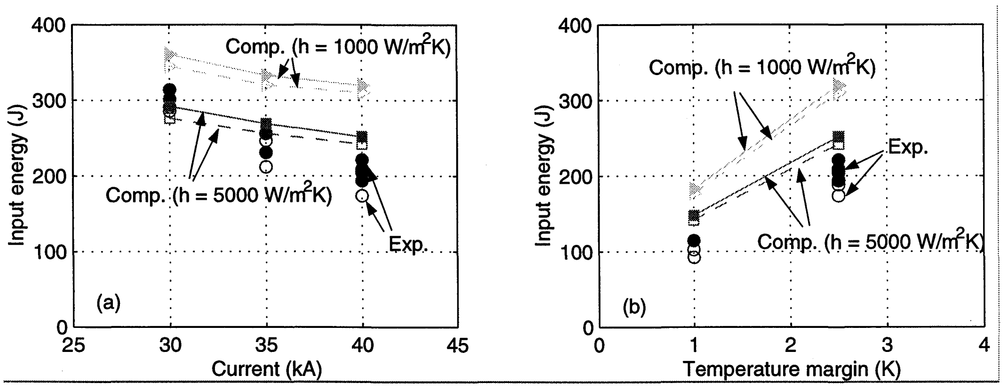

FIGURE 4. Sensitivity of Mithrandir simulation results to different assumptions for the heat transfer coefficient h between helium and solids. (a) Energy margin as a function of current @ 12 g/s, and ΔT_{margin} = 2.5 K, for h = 5000 W/m^2K and h = 1000 W/m^2K. (b) Energy margin as a function of ΔT_{margin} @ 40 kA and 12 g/s, for h = 5000 W/m^2K and h = 1000 W/m^2K.

CONCLUSION AND PERSPECTIVE

A simple electro-magnetic model of the IH has been developed and coupled to the Mithrandir code. The resulting simulations of IH-driven stability tests of the CSIC are in agreement with the experiment once reasonable parameters are chosen for the heat transfer coefficients and the IH geometry.

An improved model of the IH (full-2D with square cross section or 3D) shall be done and will be coupled to Mithrandir. This may be relevant both for the analysis of the CSIC results and for the design of future experiments (e.g., the ITER Poloidal Field Coil Insert). The preliminary sensitivity analysis on thermal-hydraulic input parameters presented here, shall also be extended in order to more precisely assess the robustness of the results of the simulation.

ACKNOWLEDGEMENTS

EFDA and MURST partially financially supported the work of RZ and LS, and LS also thanks ASP for support through a post-doctoral fellowship. RZ and LS thank JAERI for the wonderful hospitality provided during the CSIC tests, and N.Martovetsky for reading the manuscript. Data files for the heater calibration were provided by T.Isono.

REFERENCES

1. Tsuji, H., Okuno, K., Thome, R., et al., "Progress of the ITER Central Solenoid Model Coil program", *Nucl. Fusion* **41**, pp. 645-651 (2001).
2. Savoldi, L., Salpietro, E., and Zanino, R., "Inductively driven transients in the CS Insert Coil (II): Quench tests and analysis", presented at the Cryogenic Engineering Conference, July 16-20, 2001, Madison (WI) USA.
3. Isono, T., "Report on calibration of inductive heating in CS insert", JAERI memo JASC-2001-083.
4. Zanino, R., De Palo, S., and Bottura, L., "A two-fluid code for the thermohydraulic transient analysis of CICC superconducting magnets", *J. Fus. Energy* **14**, pp. 25-41 (1995).
5. Zanino, R., and Marinucci, C., "Heat slug propagation in QUELL. Part I: experimental setup and 1-fluid GANDALF analysis", *Cryogenics* **39**, pp. 585-593 (1999); Zanino, R., and Marinucci, C., "Heat slug propagation in QUELL. Part II: 2-fluid MITHRANDIR analysis", *Cryogenics* **39**, pp. 595-608 (1999).
6. Zanino, R., Bottura, L., and Marinucci, C., "Computer simulation of quench propagation in QUELL", *Adv. Cryo. Eng.* **43**, pp. 181-188 (1998); Savoldi, L., Bottura, L., and Zanino, R., "Simulation of Thermal-Hydraulic Transients in Two-Channel CICC with Self-Consistent Boundary Conditions", *Adv. Cryo. Eng.* **45**, pp. 697-704 (2000).
7. Zanino, R., Gung, C.Y., Hamada, K., and Savoldi, L., "Pressure drop analysis in the CS Insert Coil", presented at the Cryogenic Engineering Conference, July 16-20, 2001, Madison (WI) USA.
8. Bruzzone, P.L., private communication to AP (2001).
9. Zanino, R., and Savoldi, L., "Tests and Modeling of Heat Generation and Heat Exchange in the Full Size Joint Sample", Proceedings of the 18-th International Cryogenic Engineering Conference (ICEC18), pp. 363-366, Mumbai, India, 21-25 February, 2000.
10. Martovetsky, N., LLNL memo on "Assessment of the CS Insert Tcs data: how do we compare conductor performance to the strand and how we make interpretations", 5/18/2001.
11. Duchateau, J.L., "Intrinsic strain evolution in the CS Insert", presented at the 5-th EU CSMC Test&Analysis Meeting, January 31, 2001, Forschungszentrum Karlsruhe, Germany.
12. Martovetsky, N., LLNL memo on "Distribution of magnetic field in CSMC and CS Insert", 12/29/1999; Galindo, V., private communication to LS (2001).
13. Mitchell, N., "Analysis of slow temperature and current ramps on the Central Solenoid Insert Coil", *Cryogenics* **40**, pp. 605-615 (2000)
14. Seo, K., "Estimation of current redistribution after inductive heating by voltage tap signals", presented at the Meeting on CSMC and CSIC Test Results, Naka, Japan, November 9-11, 2000.